Endothelial PDGF-B retention is required for proper investment of pericytes in the microvessel wall

Per Lindblom,[1] Holger Gerhardt,[1] Stefan Liebner,[3] Alexandra Abramsson,[1] Maria Enge,[1] Mats Hellström,[4] Gudrun Bäckström,[5] Simon Fredriksson,[6] Ulf Landegren,[6] Henrik C. Nyström,[2] Göran Bergström,[2] Elisabetta Dejana,[3] Arne Östman,[5] Per Lindahl,[1] and Christer Betsholtz[1,7]

[1]Department of Medical Biochemistry and [2]Department of Physiology, Göteborg University, Göteborg SE-405 30, Sweden; [3]FIRC Institute of Molecular Oncology, Milan 20139, Italy; [4]Angiogenetics AB, Göteborg SE-405 30, Sweden; [5]Ludwig Institute for Cancer Research, Uppsala SE-751 24, Sweden; [6]The Beijer Laboratory, Department of Genetics and Pathology, Uppsala University, Uppsala SE-751 85, Sweden

Several platelet-derived growth factor (PDGF) and vascular endothelial growth factor (VEGF) family members display C-terminal protein motifs that confer retention of the secreted factors within the pericellular space. To address the role of PDGF-B retention in vivo, we deleted the retention motif by gene targeting in mice. This resulted in defective investment of pericytes in the microvessel wall and delayed formation of the renal glomerulus mesangium. Long-term effects of lack of PDGF-B retention included severe retinal deterioration, glomerulosclerosis, and proteinuria. We conclude that retention of PDGF-B in microvessels is essential for proper recruitment and organization of pericytes and for renal and retinal function in adult mice.

Received April 3, 2003; revised version accepted May 23, 2003.

The control of cell migration and the formation of specific patterns during embryonic development are believed to depend, at least in part, on the precise spatial distribution of secreted growth and differentiation factors (GDFs). This is achieved by strictly localized and regulated synthesis and secretion of GDFs, but also by binding of the secreted GDFs to cell surface- and extracellular matrix molecules. One type of molecule strongly implicated in the regulation of GDF activities in vivo is the heparan sulphate proteoglycans (HSPGs; Baeg and Perrimon 2000; Gallagher 2001; Iozzo and San Antonio 2001). HSPG-binding properties have been demonstrated for a wide range of GDFs, including members of the FGF, TGF-β, EGF, IGF, PDGF, VEGF, Wnt, and hedgehog families, as well as many chemokines and cytokines (for review, see Gallagher 2001; Iozzo and San Antonio 2001). Most likely, the negatively charged sulfate groups on the disaccharide building blocks of heparan sulfate (HS) polysaccharide chains provide binding sites for positively charged amino acid sequence motifs present in the GDFs. By binding to HSPGs, specific gradients of the GDFs may be created, which may guide or restrict morphogenetic responses (Perrimon and Bernfield 2000; Ruhrberg et al. 2002; Gerhardt et al. 2003). HSPG binding may also lead to the formation of reservoirs of factors for use in wound repair. Finally, HSPGs may act as coreceptors by stabilizing active ligand-receptor complexes (Pellegrini et al. 2000).

Certain isoforms of platelet-derived growth factor (PDGF) and vascular endothelial growth factor (VEGF) family members display positively charged stretches of amino acids residues at the C terminus. These stretches are included or excluded depending on alternative splicing or proteolytic processing (Eriksson and Alitalo 1999; Heldin and Westermark 1999). For VEGF-A, the long splice isoforms, which carry HSPG-binding domains, accumulate on the cell surface or in the extracellular matrix, whereas short VEGF-A is diffusible following cellular release (Park et al. 1993). The developmental role of HSPG binding of VEGF-A was recently addressed using mice in which the long VEGF-A splice isoforms were selectively ablated (Carmeliet et al. 1999; Ruhrberg et al. 2002; Stalmans et al. 2002). In these mice, extracellular VEGF-A distribution becomes more widespread, leading to changes in endothelial sprouting and branching, and to the formation of abnormal vascular patterns (Ruhrberg et al. 2002). In PDGF-A and PDGF-B, the HSPG-binding motifs do not affect receptor binding or biological activity of the recombinant proteins (Östman et al. 1989). However, in transfected cells, these motifs confer retention of the secreted growth factor to the surface of the producing cells. Conversely, absence of the retention motif leads to increased secretion of a diffusible protein that readily accumulates in the cell culture medium (LaRochelle et al. 1991; Östman et al. 1991; Raines and Ross 1992; Andersson et al. 1994). The retention motif also appears to limit the action range of PDGF-B in vivo, as suggested from experiments with transplanted keratinocytes transfected with PDGF-B expression vectors (Eming et al. 1999). To achieve insight into the physiological role of PDGF-B retention, we deleted the PDGF-B retention motif in mice by targeted mutagenesis, and we analyzed the phenotypic consequences of this mutation.

Results and Discussion

Generation and characterization of the pdgf-b^{ret} *allele*

To delete the PDGF-B retention motif, we targeted a loxP-flanked PGK-neo cassette into intron 5 and a premature translation stop codon/*Hin*dIII site into exon 6 of the *pdgf-b* gene in mouse embryonic stem (ES) cells (Fig. 1). Heterozygous mutants were produced and further crossed with protamine-Cre mice to delete the PGK-neo cassette, generating a *pdgf-b*^{ret} (retention motif knockout) allele. The *pdgf-b*^{ret} allele demonstrated Mendelian inheritance, and both *pdgf-b*$^{ret/+}$ (+ indicates wild type)

[*Keywords*: PDGF; cell retention; heparan sulphate proteoglycan; pericyte; mesangial cell; retina]
[7]Corresponding author.
E-MAIL Christer.Betsholtz@medkem.gu.se; FAX 46-31-416108.
Article and publication are at http://www.genesdev.org/cgi/doi/10.1101/gad.266803.

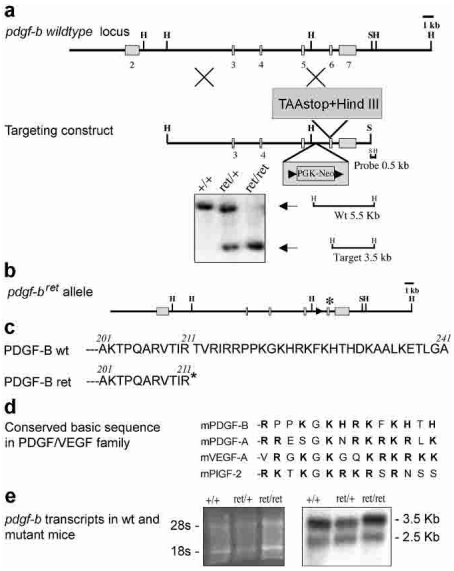

Figure 1 The *pdgf-b*^{ret} allele. (*a*) Outline of the *pdgf-b* locus, targeting construct, and Southern identification of the *pdgf-b*^{ret} allele. (*b*) Schematic outline of the *pdgf-b*^{ret} allele. Remaining loxP site and inserted TAA-stop denoted by arrowhead and asterisk, respectively. (*c*) C-terminal sequence of the predicted PDGF-Bwt and PDGF-Bret proteins. (*d*) Comparison of the retention motifs of mouse PDGF and VEGF members. Basic residues in bold. (*e*) Northern blot analysis of *pdgf-b* transcripts in *pdgf-b*$^{+/+}$, *pdgf-b*$^{ret/+}$, and *pdgf-b*$^{ret/ret}$ brains. (*Left*) EtBr-stained gel.

and *pdgf-b*$^{ret/ret}$ mice survived into adulthood. *Pdgf-b*$^{ret/ret}$ mice were slightly growth retarded and showed reduced female fertility. Northern blot analysis of brain RNA showed similar size *pdgf-b* transcripts but approximately twofold reduced levels in *pdgf-b*$^{ret/ret}$ mice compared to *pdgf-b*$^{+/+}$ mice (Fig. 1e). Expression of the *pdgf-b*^{ret} allele was also verified in the brain by reverse transcriptase PCR (RT–PCR) followed by diagnostic *Hin*dIII cleavage at the *pdgf-b*^{ret} premature stop codon (data not shown).

Recombinant PDGF-B lacking the C-terminal retention motif has full biological activity (Östman et al. 1989) and is more efficiently released from transfected cells than wild-type PDGF-B (LaRochelle et al. 1991; Östman et al. 1991; Raines and Ross 1992; Andersson et al. 1994; Eming et al. 1999). We therefore expected a dominant effect of a potentially hyperfunctional *pdgf-b*^{ret} allele. However, genetic data suggested that the *pdgf-b*^{ret} allele was *hypo*-functional; *pdgf-b*$^{ret/+}$ mice were indistinguishable from *pdgf-b*$^{+/+}$ or *pdgf-b*$^{+/-}$ mice, and *pdgf-b*$^{ret/-}$ mice were perinatal lethal like *pdgf-b*$^{-/-}$ mice (Levéen et al. 1994). Because the most important site for PDGF-B expression during development is the microvascular endothelium (Lindahl et al. 1997; Enge et al. 2002), we analyzed the expression of the *pdgf-b*^{ret} allele in endothelial cells. In situ hybridization of flat-mounted retinas showed that expression of the *pdgf-b*$^{+}$ transcript was concentrated to endothelial cells situated at the tips of the vascular sprouts (Fig. 2a,c). This confirmed the recent identification of *pdgf-b* mRNA as a marker for endothelial tip-cells (Gerhardt et al. 2003). The *pdgf-b*^{ret} signal had a similar distribution (Fig. 2b,d), but was weaker than the *pdgf-b*$^{+}$ signal, in agreement with the Northern data. To analyze the function and distribution of endogenous PDGF-Bret protein from endothelial cells, we established immortalized polyoma virus-transformed endothelioma cells lines from wild-type and *pdgf-b*$^{ret/ret}$ mice. Both lines expressed similar-sized *pdgf-b* transcripts, but the levels were threefold lower in *pdgf-b*$^{ret/ret}$ cells (data not shown). PDGF-B protein expression in the endothelioma lines was too low to be detected by metabolic labeling or Western blotting (data not shown). This was not unexpected, because prior attempts have failed to detect PDGF-B protein expressed from the endogenous *pdgf-b* gene by these methods; the only published examples of PDGF-B protein visualized by, for example, immunoprecipitation have utilized transfected cells. We therefore analyzed PDGF-B protein levels in conditioned media and cell lysates using a sensitive and specific method (Fredriksson et al. 2002) involving PDGF-B-binding aptamers and proximity-dependent DNA ligation (Fig. 2e). Conditioned media were also analyzed for activity in a PDGF β-receptor (PDGFR-β) tyrosine phosphorylation assay (Fig. 2g). Both assays demonstrated lower PDGF-B levels in *pdgf-b*$^{ret/ret}$ cells compared to *pdgf-b*$^{+/+}$ cells. The two different assays yielded comparable results (~0.1 or 0.15 ng/mL, respectively in *pdgf-b*$^{ret/ret}$ samples, and ~0.5 and 0.75 ng/mL, in *pdgf-b*$^{+/+}$ samples), confirming that the PDGF-Bret protein had intact PDGF receptor-binding and activating properties. The ratio between the PDGF-B content in medium versus lysate was significantly higher for the *pdgf-b*$^{ret/ret}$ than for the wild-type samples, suggesting that the PDGF-Bret protein is more efficiently released from the cells (Fig. 2f).

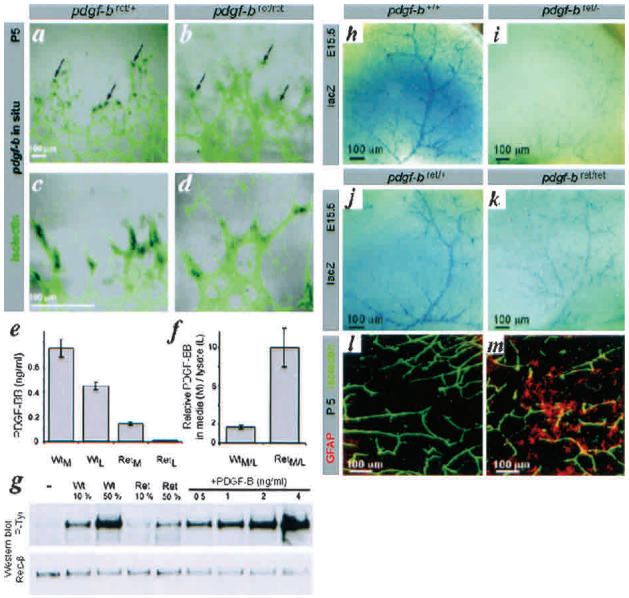

Figure 2. Expression of the *pdgf-b*^{ret} allele, activity of the PDGF-Bret protein, and deficient recruitment of pericytes in *pdgf-b*$^{ret/ret}$ mice. (*a–d*) In situ hybridization localizes *pdgf-b* mRNA to endothelial tip cells (arrows). (*e,f*) PDGF-B protein levels by proximity ligation assay in medium (M) and lysates (L) of wild-type (Wt) and *pdgf-b*$^{ret/ret}$ (Ret) endothelioma cell lines. Triplicate measurements are shown with standard deviations. (*g*) PDGFR-β phosphorylation induced by the indicated dilutions (%) of 10× concentrated media from endothelioma cells. Western blots with phospho-tyrosine (P-tyr) and PDGFR-β (Rec-β) antibodies are shown. (*h–k*) XlacZ4 staining of forebrain from E15.5 *pdgf-b*$^{+/+}$, *pdgf-b*$^{ret/+}$, *pdgf-b*$^{ret/ret}$, and *pdgf-b*$^{ret/-}$ mice. LacZ-positive pericytes and vSMCs align cerebral/meningeal vessels. (*l,m*) GFAP (red) and isolectin (green) staining of P5 vibratome-sectioned brain. Up-regulation of GFAP in astrocytes is seen in focal regions of the *pdgf-b*$^{ret/ret}$ brain.

Pdgf-b$^{ret/ret}$ show impaired mice pericyte investment into the microvessel wall

In developing mouse embryos, PDGF-B expression is largely restricted to endothelial cells, whereas PDGFR-β expression occurs in vascular smooth muscle cells and pericytes (Lindahl et al. 1997). Analyses of knock-out mice for PDGF-B and PDGFR-β have shown that PDGF-B signaling via PDGFR-β is critically involved in recruitment of pericytes and vascular smooth muscle cells (vSMCs) to blood vessels (Lindahl et al. 1997; Hellström et al. 1999, 2001). To analyze pericyte densities in *pdgf-b*$^{ret/ret}$ mice, we bred them onto the XlacZ4 background, which allows simple quantification of pericyte densities in whole-mount CNS preparations (Tidhar et al. 2001). At embryonic day 15.5 (E15.5), the number of pericytes in the forebrain was reduced to ~50% of normal in *pdgf-b*$^{ret/ret}$ mice, and even further in *pdgf-b*$^{ret/-}$ (~25% of normal; Fig. 2h–k) and *pdgf-b*$^{-/-}$ mice (<5% of normal; data not shown). The pericyte deficiency in *pdgf-b*$^{ret/ret}$ mice was confirmed using α-smooth muscle actin (SMA) and NG2 proteoglycan staining (data not shown). The reduction in brain pericyte density correlated with abnormal capillary morphology and focal reactive gliosis in postnatal mice, likely reflecting persistent microvascular dysfunction (Fig. 2l,m).

PDGF-B controls pericyte proliferation (Hellström et al. 1999), but may also stimulate pericyte migration along the developing microvessels. Because the *pdgf-b*^{ret} allele is hypomorphic at the levels of mRNA and protein expression, the observed reduction in pericyte numbers in *pdgf-b*$^{ret/ret}$ mice was expected. Previously analyzed hypomorphic situations include *Pdgf-b*$^{+/-}$ mice, which show an ~30% reduction in retinal pericyte density (Hammes et al. 2002), and compound *pdgf-b*$^{+/-}$, *pdgfr-β*$^{+/-}$ heterozygotes, which show an ~50% reduction (A. Lundkvist and C. Betsholtz, unpubl.). We have also generated endothelium-restricted PDGF-B knockouts (*pdgf-b*$^{lox/-}$ mice; Enge et al. 2002), which vary in their degree of interindividual chimerism for the recombined PDGF-B allele, producing a range of PDGF-B-deficient states with up to 90% reduction in pericyte density in the most severely affected individuals (Enge et al. 2002). Because these mice were viable, the lethality of *pdgf-b*$^{ret/-}$ mice and the severity of the *pdgf-b*$^{ret/ret}$ phenotype (see below) appeared worse than expected from the observed reduction in pericyte density only. We therefore investigated in more detail the association between the pericytes and the endothelial cells in *pdgf-b*$^{ret/ret}$ mice.

Pericytes normally extend dendritic processes that associate intimately with the abluminal endothelial surface (for review, see Allt and Lawrenson 2001). High-resolution imaging of pericytes using NG2 staining and confocal microscopy confirmed such association in both sprouting and mature vessels in *pdgf-b*$^{+/+}$ mice (Fig. 3e). In *pdgf-b*$^{ret/ret}$ mice, however, the pericytes were partially dissociated from the abluminal endothelial surface and protruded cellular processes away from the vessel (Fig. 3f, arrows). Similar dissociation of pericytes from the endothelial cells was observed in neovessels of tumors transplanted to *pdgf-b*$^{ret/ret}$ mice (A. Abramsson, P. Lindblom, and C. Betsholtz, unpubl.). However, the extensively hypomorphic situation created in *pdgf-b*$^{lox/-}$ mice (Enge et al. 2002) did not result in apparent pericyte detachment. The sparse pericytes in these mice extended long and thin processes that remained tightly associated with the abluminal endothelial surface (Fig. 3b,d). The inactivation of the floxed *pdgf-b* allele in these mice is, however, not complete, but rather results in a chimeric situation in which a variable proportion of the endothelial cells retain expression of PDGF-Bwt protein from a single unrecombined *pdgf-b* allele (Enge et al. 2002). Apparently, this is sufficient to render the pericytes tightly associated with the abluminal endothelial surface.

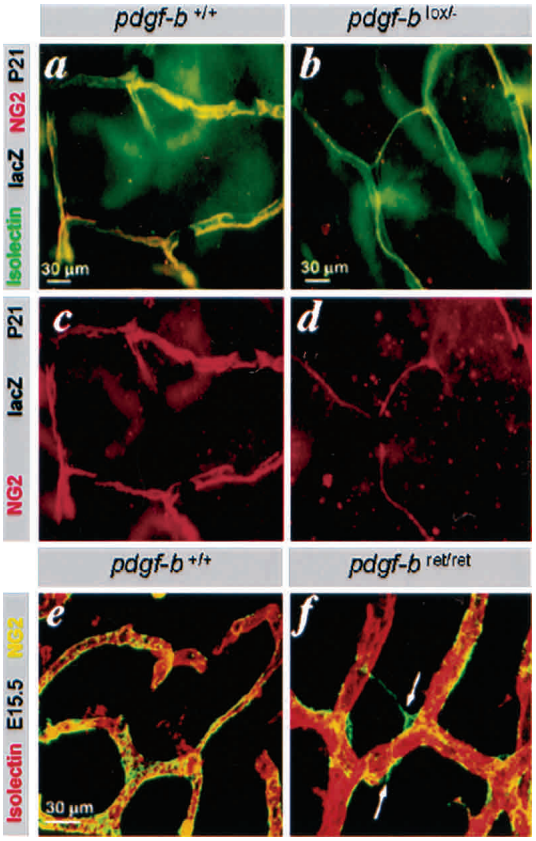

Figure 3. Defective investment of pericytes into the vessel wall in *pdgf-b*$^{ret/ret}$ mice. (*a–d*) Isolectin (green), NG2 (red), and LacZ stain of *pdgf-b*$^{+/+}$ and *pdgf-b*$^{lox/-}$ P21 retinas. The few pericytes seen in *pdgf-b*$^{lox/-}$ mice extend thin endothelium-associated processes. (*e,f*) NG2 and isolectin staining of E12.5 hindbrain. Pericytes (green) are partially detached and extend processes away from the endothelial cells (red; arrows) in *pdgf-b*$^{ret/ret}$ mice.

Severe postnatal glomerular and retinal defects in pdgf-b$^{ret/ret}$ *mice*

PDGF-B and PDGFRβ are critically involved in mesangial cell recruitment to kidney glomeruli (Levéen et al. 1994; Soriano 1994). *Pdgf-b*$^{ret/ret}$ embryos displayed a marked reduction in the number of mesangial cells in glomeruli at late gestation, leading to the formation of ballooning glomerular capillaries (Fig. 4a,b). This defect was similar to, but slightly milder than, those seen in *pdgf-b*$^{-/-}$ and *pdgfr-β*$^{-/-}$ embryos (data not shown). The mesangial cell deficiency was temporary, and by 1 mo of age, most glomeruli had normalized (Fig. 4c,d; data not shown). By 6 mo of age, however, the picture was again pathological; extensive accumulation of extracellular matrix was revealed by PAS (Fig. 4e,f) and collagen (data not shown) staining. Albuminuria was apparent in most

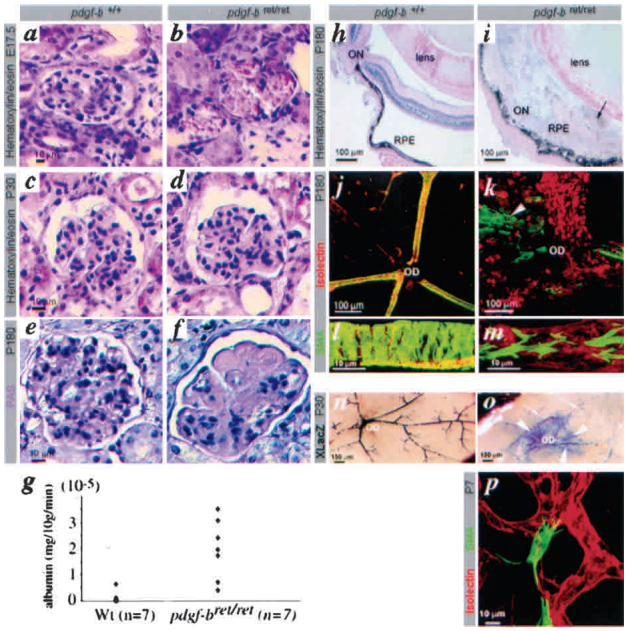

Figure 4. Glomerulosclerosis, proteinuria, retinopathy, and vSMC deficiency in *pdgf-b*$^{ret/ret}$ mice. H&E staining shows lack of mesangial cells in *pdgf-b*$^{ret/ret}$ mice at E17.5 (*a*,*b*), normal histology at P30 (*c*,*d*), and glomerulosclerosis, by PAS staining at P180 (*e*,*f*). (*g*) Albuminuria in *pdgf-b*$^{ret/ret}$ mice at 3 mo of age. (*h–p*) Analysis of postnatal retinas (P7–P180). (*h–i*) Retinal disorganization in *pdgf-b*$^{ret/ret}$ mice, with fibrosis and invasion of RPE (arrow). (*j*,*k*) Isolectin (red) and SMA (green) staining of flat-mounted mouse retinas. Arrowhead indicates area of SMA-positive cells outside vessel walls. (*l*,*m*) Different density and organization of arterial SMCs in *pdgf-b*$^{+/+}$ and *pdgf-b*$^{ret/ret}$ retinas. (*n*,*o*) XlacZ4 staining of P30 retinas shows defective pericyte recruitment in *pdgf-b*$^{ret/ret}$ mice and formation of vSMC sheets (arrowheads). (*o*) Arrows point at residual vessel-associated pericytes in peripheral regions. (*p*) Retina of P7 *pdgf-b*$^{ret/ret}$ mouse with SMA-positive pericyte partially detached from the endothelium. ON, optic nerve; OD, optic disc.

pdgf-b$^{ret/ret}$ mice at 3 mo (Fig. 4g), implicating renal dysfunction before the development of advanced glomerulosclerosis.

Macroscopic examination revealed white ocular opacities in ~10%, and small eyes in 100%, of adult *pdgf-b*$^{ret/ret}$ mice. Histological analysis revealed extensive retinal changes in all *pdgf-b*$^{ret/ret}$ individuals, including degeneration of nuclear and photoreceptor layers, invasion of retinal pigment epithelial cells (RPEs), fibrosis, and traction (Fig. 4h,i). The retinal vasculature was severely disorganized. SMA- and XlacZ4-positive cells did not invest the vascular walls appropriately (Fig. 4j–o), but instead formed cellular sheets on the retinal surface (Fig. 4k,o arrowheads). Vessel-associated vSMCs were present, but abnormally organized (Fig. 4m), and pericytes were partially detached from the endothelium (Fig. 4p). The latter coincided with up-regulated SMA expression, which is normally undetectable in the retinal pericytes, implicating altered cell differentiation.

To explore the development of the retinal pathology, we analyzed newborn *pdgf-b*$^{ret/ret}$ mice. Retinal vessels normally begin to sprout from the optic disc on postnatal day 1 (P1) and reach the retinal margin on P7. Astrocytes appear in the retina before vascularization, and are known to regulate retinal angiogenesis (Gerhardt et al. 2003). *Pdgf-b*$^{ret/ret}$ mice showed normal astrocyte patterns (data not shown), but the retinal vessels were abnormal from the onset of sprouting. Plexus formation was delayed and asymmetric at P2 (data not shown). The vascular plexuses at P5 were highly irregular and displayed fewer sprouts (Fig. 5c,k) and sites with increased (Fig. 5g) as well as decreased (Fig. 5c,k) vascular density. Vascular remodeling occurred, but the pattern of remodeled vessels was abnormal, with a notable shortage of branch points (Fig. 5g). In *pdgf-b*$^{+/+}$ and *pdgf-b*$^{ret/+}$ mice, pericytes distributed across the entire vascular plexus at all ages analyzed (Fig. 5b,f,j,n). In *pdgf-b*$^{ret/ret}$ mice, however, the abnormal retinal plexuses showed significant reduction in pericyte density, as revealed by both XlacZ4 and NG2 staining (Fig. 5d,h,l,p).

PDGF/VEGF retention and migration of vascular cells

Because it is unlikely that the retention motif in PDGF-B has a direct role in PDGF receptor binding, a more plausible explanation for the observed effects, also supported by published in vitro data, is that the retention motif helps localizing secreted PDGF-B to proteins or proteoglycans on the endothelial cell surface or in the perivascular matrix, thereby promoting its recognition by neighboring receptor-carrying cells, that is, the PDGFR-β-positive pericytes. PDGF receptor activation by immobilized or less readily diffusible PDGF-B protein may also potentially limit receptor down-regulation, thereby producing a more sustained signal. Such a scenario has been implicated for FGFs (Delehedde et al. 2000), and indi-

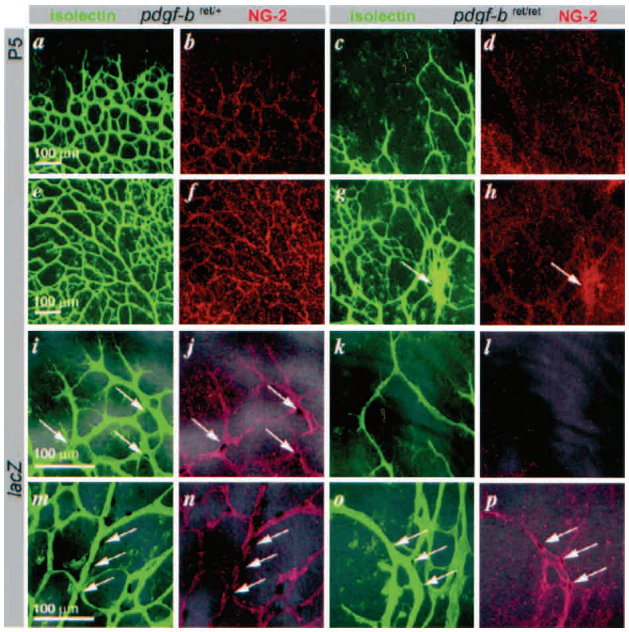

Figure 5. Retinal vascular development in *pdgf-b*$^{ret/ret}$ mice. Retinal vessels in control (*pdgf-b*$^{ret/+}$) and *pdgf-b*$^{ret/ret}$ mice at P5. EC, isolectin (green); pericytes, NG2 (red); pericyte nuclei, XlacZ4 (dark blue, arrows). Peripheral (*a*,*b*) and central (*e*,*f*) regions in *pdgf-b*$^{ret/+}$ mice show formation of regular vascular plexuses. Note extensive coverage with pericytes (*b*,*f*), except for sprouting tips (*b*). In *pdgf-b*$^{ret/ret}$ mice, plexus spreading is delayed (*c*; peripheral), and irregular (*g*; central) with regions of hyperfusion (*g*, arrow), and reduced pericyte density (*d*,*h*). Peripheral (*i–l*) and central (*m–p*) regions at high magnification show that peripheral sprouting is sparse in *pdgf-b*$^{ret/ret}$ mice, leading to a wide-meshed, irregular vasculature partially devoid of pericytes. Few pericytes are present on remodeling arteries (cf. *n* and *p*, arrows).

rectly also for PDGF-stimulated cell proliferation (Westermark and Heldin 1985) in vitro.

The effects observed in *pdgf-b*$^{ret/ret}$ mice go beyond those seen in the hypomorphic situations obtained in *pdgf-b*$^{+/-}$, *pdgfr*-β$^{+/-}$, and *pdgf-b*$^{lox/-}$ mice. The finding that pericytes were partially detached and often extended their dendritic processes away from the vessels suggests that PDGF-B retention is required for the formation of depots or gradients of the factor, which help confining pericyte migration to restricted paths—the abluminal microvessel surfaces. An analogous scenario has been proposed for VEGF-A, for which extracellular retention shapes depots or gradients that stimulate directed endothelial cell migration along astrocytes (Gerhardt et al. 2003).

Critical roles of PDGF-B and PDGFR-β in the retina and kidney glomeruli

The grossly abnormal retinal and glomerular vascular patterns in *pdgf-b*$^{ret/ret}$ mice reported here and in other genetic or pharmacological models of PDGF-B and PDGFR-β signaling deficiency (Levéen et al. 1994; Soriano 1994; Klinghoffer et al. 2001; Enge et al. 2002; Sano et al. 2002; Uemura et al. 2002) suggest a crucial function for PDGF-B/PDGFRβ signaling at these sites. In some of these models, pericyte recruitment is also abrogated at other sites, with less dramatic consequences for organ histology and function. This pattern of organ sensitivity to pericyte deficiency may be relevant in the context of diabetes. Defects in retinal pericytes and renal mesangial cells are hallmarks of diabetic microangiopathy, but their cause(s) and consequence(s) are unclear. Further studies using *pdgf-b*$^{ret/ret}$ mice and other PDGF-B and PDGFR-β-deficient models may help clarify the roles of pericytes and mesangial cells in this disease.

Materials and methods

Generation and analysis of pdgf-b$^{ret/ret}$*-deficient mice*

A targeting construct encompassing the 3′ region of the *pdgf-b* gene was generated with a premature translation stop codon inserted in exon 6 (amino acid position 211; see Fig. 1) by site-directed mutagenesis using the Altered Sites II In Vitro Mutagenesis System Q6210 (Promega). After sequence verification, the targeting construct was linearized with *Not*I and transfected into R1 ES cells. Correctly targeted ES cell clones were identified (Fig. 1) and used to generate germline *pdgf-b*^{ret} mutants using previously described protocols (Levéen et al. 1994). PolyA$^+$RNA isolation and Northern blotting were done using RNeasy midiprep, Oligotex mRNA (QIAGEN), and Northern Max (Ambion) kits. For in situ hybridization, eyes were dissected in ice-cold 4% paraformaldehyde (PFA) and processed as described (Fruttiger 2002). Immunohistochemistry on retinas was performed as described (Gerhardt et al. 2003). Other mouse tissues were fixed in 4% PFA, paraffin-embedded, sectioned, and stained using standard protocols. For urine sampling, mice were placed in metabolic cages and urine collected during a 24-h period (volume range 1–3 mL). Ten-microliter samples were diluted and assayed by ELISA using AlbuwellM kits (Exocell) according to the manufacturer's instructions.

Endothelioma cultures

Endothelial cells were isolated from lungs of adult *pdgf-b*$^{ret/ret}$ and control mice and cultured as described (Allavena et al. 1995). After 2–3 d, the cells were infected with polyoma virus (Bussolino et al. 1991). Cells were routinely cultured in MCDB131 (Invitrogen) supplemented with 15% fetal calf serum (Hyclone), endothelial cell growth supplement 50 µg/mL (Sigma), heparin 100 µg/mL (Sigma), glutamine, and antibiotics on gelatin-coated tissue culture dishes. Serum-free media conditioned for 24 h by subconfluent cultures of *pdgf-b*$^{+/+}$ and *pdgf-b*$^{ret/ret}$ endothelioma cells were collected and concentrated to 10% of the original volume using Centriplus filter devices (Amicon). Cell-lysates were generated (Pietras et al. 2002), and receptor phosphorylation was determined using cells stably transfected with PDGF β-receptor as described (Pietras et al. 2001). PDGF-B concentrations were analyzed by homogenous proximity ligation as described (Fredriksson et al. 2002). The real-time PCR reactions following ligation where performed using a modified protocol (S. Fredriksson and U. Landegren, unpubl.).

Acknowledgments

We acknowledge Göteborg University TCF for transgenic services and Moshe Shani for XlacZ4 transgenic mice. Grants were donated by the Novo Nordisk Foundation, the Swedish Cancer Foundation, and the Inga Britt and Arne Lundberg Foundation. S.F. was supported by the Beijer Foundation.

The publication costs of this article were defrayed in part by payment of page charges. This article must therefore be hereby marked "advertisement" in accordance with 18 USC section 1734 solely to indicate this fact.

References

Allavena, P., Dejana, E., Bussolino, F., Vecchi, A., and Mantovani, A. 1995. Cytokine regulation of endothelial cells. In *Cytokines: A practical approach* (ed. F.R. Balkwill), pp. 225–245. IRL Press, Oxford.

Allt, G. and Lawrenson, J.G. 2001. Pericytes: Cell biology and pathology. *Cells Tissues Organs* **169:** 1–11.

Andersson, M., Ostman, A., Westermark, B., and Heldin, C.H. 1994. Characterization of the retention motif in the C-terminal part of the long splice form of platelet-derived growth factor A-chain. *J. Biol. Chem.* **269:** 926–9330.

Baeg, G.H. and Perrimon, N. 2000. Functional binding of secreted molecules to heparin sulphate proteoglycans in *Drosophila*. *Curr. Opin. Cell Biol.* **12:** 575–580.

Bussolino, F., De Rossi, M., Sica, A., Colotta, F., Wang, J.M., Bocchietto, E., Padura, I.M., Bosia, A., Dejana, E., and Mantovani, A. 1991. Murine endothelioma cell lines transformed by polyoma middle T oncogene as target for and producers of cytokines. *J. Immunol.* **147:** 2122–2129.

Carmeliet, P., Ng, Y.S., Nuyens, D., Theilmeier, G., Brusselmans, K., Cornelissen, I., Ehler, E., Kakkar, V.V., Stalmans, I., Mattot, V., et al. 1999. Impaired myocardial angiogenesis and ischemic cardiomyopathy in mice lacking the vascular endothelial growth factor isoforms VEGF164 and VEGF188. *Nat. Med.* **5:** 495–502.

Delehedde, M., Seve, M., Sergeant, N., Wartelle, I., Lyon, M., Rudland, P.S., and Fernig, D.G. 2000. Fibroblast growth factor-2 stimulation of p42/44MAPK phosphorylation and IκB degradation is regulated by heparan sulfate/heparin in rat mammary fibroblasts. *J. Biol. Chem.* **275:** 33905–33910.

Eming, S.A., Yarmush, M.L., Krueger, G.G., and Morgan, J.R. 1999. Regulation of the spatial organization of mesenchymal connective tissue: Effects of cell-associated versus released isoforms of platelet-derived growth factor. *Am. J. Pathol.* **154:** 281–289.

Enge, M., Bjarnegård, M., Gerhardt, H., Gustafsson, E., Kalén, M., Asker, N., Hammes, H.-P., Shani, M., Fässler, R., and Betsholtz, C. 2002. Endothelium-specific platelet-derived growth factor-B ablation mimics diabetic retinopathy. *EMBO J.* **21:** 4307–4316.

Eriksson, U. and Alitalo, K. 1999. Structure, expression, and receptor-binding properties of novel vascular endothelial growth factors. *Curr. Top. Microbiol. Immunol.* **237:** 41–57.

Fredriksson, S., Gullberg, M., Jarvius, J., Olsson, C., Pietras, K., Gustafsdottir, S.M., Östman, A., and Landegren, U. 2002. Protein detection using proximity-dependent DNA ligation assays. *Nat Biotechnol.* **20:** 473–477.

Fruttiger, M. 2002. Development of the mouse retinal vasculature: Angiogenesis versus vasculogenesis. *Invest. Opthalmol. Vis. Sci.* **43:** 522–527.

Gallagher, J.T. 2001. Heparan sulfate: Growth control with a restricted menu. *J. Clin. Invest.* **108:** 357–361.

Gerhardt, H., Golding, M., Fruttiger, M., Ruhrberg, C., Lundkvist, A., Abramsson, A., Jeltsch, M., Mitchell, C., Alitalo, K., Shima, D., et al. 2003. VEGF guides angiogenic sprouting utilizing endothelial tip-cell

filopodia. *J. Cell Biol.* **161:** 1163–1177. (Published online ahead of print June 16, 2003 as 10.1083/jcb.200302047.)
Hammes, H.-P., Lin, J., Renner, O., Shani, M., Lundqvist, A., Betsholtz, C., Brownlee, M., and Deutsch, U. 2002. Pericytes and the pathogenesis of diabetic retinopathy. *Diabetes* **51:** 3107–3112.
Heldin, C.H. and Westermark, B. 1999. Mechanism of action and in vivo role of platelet-derived growth factor. *Physiol. Rev.* **79:** 1283–1316.
Hellström, M., Kalén, M., Lindahl, P., Abramsson, A., and Betsholtz, C. 1999. Role of PDGF-B and PDGFR-β in recruitment of vascular smooth muscle cells and pericytes during embryonic blood vessel formation in the mouse. *Development* **126:** 3047–3055.
Hellström, M., Gerhardt, H., Kalén, M., Li, X., Eriksson, U., Wolburg, H., and Betsholtz, C. 2001. Lack of pericytes leads to endothelial hyperplasia and abnormal vascular morphogenesis. *J. Cell Biol.* **153:** 543–553.
Iozzo, R.V. and San Antonio, J.D. 2001. Heparan sulfate proteoglykans: Heavy hitters in the angiogenesis arena. *J. Clin. Invest.* **108:** 349–355.
Klinghoffer, R.A., Mueting-Nelsen, P.F., Faerman, A., Shani, M., and Soriano, P. 2001. The two PDGF receptors maintain conserved signaling in vivo despite divergent embryological functions. *Mol. Cell* **7:** 343–354.
LaRochelle, W.J., May-Siroff, M., Robbins, K.C., and Aaronson, S.A. 1991. A novel mechanism regulating growth factor association with the cell surface: Identification of a PDGF retention domain. *Genes & Dev.* **5:** 1191–1199.
Levéen, P., Pekny, M., Gebre-Medhin, S., Swolin, B., Larsson, E., and Betsholtz, C. 1994. Mice deficient for PDGF B show renal, cardiovascular, and hematological abnormalities. *Genes & Dev.* **8:** 1875–1887.
Lindahl, P., Johansson, B.R., Levéen, P., and Betsholtz, C. 1997. Pericyte loss and microaneurysm formation in PDGF-B-deficient mice. *Science* **277:** 242–245.
Östman, A., Bäckström, G., Fong, N., Betsholtz, C., Wernstedt, C., Hellman, U., Westermark, B., Valenzuela, P., and Heldin, C.-H. 1989. Expression of three recombinant homodimeric isoforms of PDGF in *Saccharomyces cerevisiae*: Evidence for difference in receptor binding and functional activities. *Growth Factors* **1:** 271–281.
Östman, A., Andersson, M., Betsholtz, C., Westermark, B., and Heldin, C.-H. 1991. Identification of a cell retention signal in the B-chain of PDGF and in the long splice version of the A-chain. *Cell Regul.* **2:** 503–512.
Park, J.E., Keller, G.A., and Ferrara, N. 1993. The vascular endothelial growth factor (VEGF) isoforms: Differential deposition into the subendothelial extracellular matrix and bioactivity of extracellular matrix-bound VEGF. *Mol. Biol. Cell* **4:** 1317–1326.
Pellegrini, L., Burke, D.F., von Delft, F., Mulloy, B., and Blundell, T.L. 2000. Crystal structure of fibroblasts growth factor receptor ectodomain bound to ligand and heparin. *Nature* **407:** 1029–1034.
Perrimon, N. and Bernfield, M. 2000. Specificities of heparan sulphate proteoglycans in developmental processes. *Nature* **404:** 725–728.
Pietras, K., Östman, A., Sjöquist, M., Buchdunger, E., Reed, R.K., Heldin, C.-H., and Rubin, K. 2001. Inhibition of platelet-derived growth factor receptors reduces interstitial hypertension and increases transcapillary transport in tumors. *Cancer Res.* **61:** 5778–5783.
Pietras, K., Rubin, K., Sjoblom, T., Buchdunger, E., Sjoquist, M., Heldin, C.-H., and Östman, A. 2002. Inhibition of PDGF receptor signaling in tumor stroma enhances antitumor effect of chemotherapy. *Cancer Res.* **62:** 5476–5484.
Raines, E.W. and Ross, R. 1992. Compartmentalization of PDGF on extracellular binding sites dependent on exon-6-encoded sequences. *J. Cell Biol.* **116:** 533–543.
Ruhrberg, C., Gerhardt, H., Golding, M., Watson, R., Ioannidou, S., Fujisawa, H., Betsholtz, C., and Shima, D. 2002. Spatially restricted patterning cues provided by heparin-binding VEGF-A control blood vessel branching morphogenesis. *Genes & Dev.* **16:** 2684–2698.
Sano, H., Ueda, Y., Takakura, N., Takemura, G., Doi, T., Kataoka, H., Murayama, T., Xu, Y., Sudo, T., Nishikawa, S., et al. 2002. Blockade of platelet-derived growth factor receptor-β pathways induces apoptosis of vascular endothelial cells and disrupts glomerular capillary formation in neonatal mice. *Am. J. Pathol.* **161:** 135–143.
Soriano, P. 1994. Abnormal kidney development and hematological disorders in PDGF β-receptor mutant mice. *Genes & Dev.* **8:** 1888–1896.
Stalmans, I., Yin-Shan, N., Rohan, R., Fruttiger, M., Bouché, A., Ÿuce, A., Fijusawa, H., Hermans, B., Shani, M., Jansen, S., et al. 2002. Arteriolar and venolar patterning in retinas of mice selectively expressing VEGF isoforms. *J. Clin. Invest.* **109:** 327–336.
Tidhar, A., Reichenstein, M., Cohen, D., Faerman, A., Copeland, N.G., Gilbert, D.J., Jenkins, N.A., and Shani, M. 2001. A novel transgenic marker for migrating limb muscle precursors and for vascular smooth muscle cells. *Dev. Dyn.* **220:** 60–73.
Uemura, A., Ogawa, M., Hirashima, M., Fujiwara, T., Koyama, S., Takagi, H., Honda, Y., Wiegand, S.J., Yancopoulos, G.D., and Nishikawa, S. 2002. Recombinant angiopoietin-1 restores higher-order architecture of growing blood vessels in mice in the absence of mural cells. *J. Clin. Invest.* **110:** 1619–1628.
Westermark, B. and Heldin, C.-H. 1985. Similar action of platelet-derived growth factor and epidermal growth factor in the prereplicative phase of human fibroblasts suggests a common intracellular pathway. *J. Cell. Physiol.* **124:** 43–48.